

Cotton immune responses are regulated by miR398b in response to the fungus *Verticillium dahliae*

Yuhuan Miao¹, Kun Chen¹, Jinwu Deng², Lin Zhang³, Muhammad Shaban¹, Xinhui Nie¹, Chunyuan You¹, Steven J. Klosterman¹, Xianlong Zhang⁴, and Longfu Zhu³

¹Affiliation not available

²National Key Laboratory of Crop Genetic Improvement, Huazhong Agricultural University

³Huazhong Agriculture University

⁴Huazhong Agricultural University

May 5, 2020

Abstract

MicroRNAs play essential roles during defense responses in plants, yet their roles have not been widely functionally validated in cotton response to *Verticillium dahliae*. Here, we employed transgenic technology, virus induced gene silencing technology, as well as various cytological and molecular tools to investigate the function of miR398b and its target genes in cotton response to *V. dahliae*. Transcript levels of miR398b were down-regulated by *V. dahliae* infection and miR398b overexpression in cotton made the plants more susceptible to *V. dahliae*. The results suggest that miR398b negatively regulates cotton resistance to *V. dahliae* via two possibilities. One is that miR398b may repress some CC-NBS-LRR genes during transcriptional or translational processes, thereby interfering with defense responses of cotton to *V. dahliae* and causing increased susceptibility of cotton to *V. dahliae*. Another possibility is that miR398b may guide the cleavage of the mRNAs of GhCSD1, GhCSD2 and GhCCS, which are important in the regulation of ROS homeostasis, thereby leading to excessive ROS accumulation in miR398b-overexpressing plants during *V. dahliae* infection. These studies illuminate the conserved and novel roles of miR398b during the cotton-*V. dahliae* interaction, which yields insights into new strategies to improve resistance to *V. dahliae* in cotton breeding programs

Verticillium dahliae

SIGNIFICANCE STATEMENT

Our study reveals that miR398b negatively regulates *V. dahliae* resistance in cotton by modulating the expression of *NBS-LRR* genes to suppress defense signaling and regulate transcript levels of superoxide dismutase to influence ROS homeostasis.

INTRODUCTION

Cotton (*Gossypium* spp.) cultivation has a major impact in human society since it is widely used as a source of fiber and seed oil. *Verticillium* wilt disease caused by the soil-borne vascular disease *Verticillium dahliae* is one of the major threats limiting cotton productivity. Diseased cotton is characterized by wilting, stunting, chlorosis, vascular discoloration, early senescence (Xu et al., 2013). Strains of *V. dahliae* isolated from cotton have been characterized as causing a defoliating or non-defoliating phenotype, and the genetic basis for the defoliating phenotype was recently established (Zhang et al. 2019). In either case, there are few resistant germplasm sources or efficient management measures available to control this pathogen, especially post-infection. *Verticillium dahliae* has a very broad host range, infecting over 200 plant species, and survives for years in the soil, precluding crop rotation as a strategy for disease control (Klosterman et al. 2009).

The evolutionary arms race between plants and pathogens has prompted the development of innate immune responses. One of these immune responses is known as MAMP (microbe-associated molecular pattern)-triggered immunity (MTI), and this response serves as the first barrier to guard against the invasion of pathogens (Chisholm et al., 2006). Another immune response is known as effector-triggered immunity (ETI), which is carried out by dominant resistance (R) proteins by recognizing pathogen effector proteins directly or indirectly, to trigger gene-for-gene resistance (Jones and Dangl, 2006). The canonical R proteins contain a nucleotide binding site (NBS) and leucine-rich repeat (LRR) domains. The core nucleotide binding domain in NBS-LRR proteins is known as the NB-ARC domain since it is well studied in APAF-1 (apoptotic protease-activating factor-1), R proteins, and CED-4 (*Caenorhabditis elegans* death-4 protein) (van der Biezen and Jones, 1998). In plants, NBS-LRR proteins mediate pathogen-specific effector triggered immunity, and the genes that encode them are widely used as markers in plant breeding to generate disease resistance. A drawback of R-mediated resistance is that it occurs at the expense of fitness (Tian et al., 2003), which suggests that the expression of an R gene must be highly regulated, and strictly inactivated in the absence of a pathogen.

Reactive oxygen species (ROS) also play multiple roles in MTI and ETI defense. For example, ROS can function as secondary messengers directly or indirectly to activate the expression of defense-related genes and induce programmed cell death during the hypersensitive response (HR) (Mittler, 2017; Mittler et al., 2011). However, excessive ROS adversely affects many cellular functions by causing oxidative damage to DNA, RNA, proteins and membranes (Apel and Hirt, 2004). Plants have evolved many antioxidative systems to eliminate ROS, including enzymatic and nonenzymatic mechanisms. Enzymatic ROS scavenging mechanisms in plants include superoxide dismutase (SOD), glutathione peroxidase (GPX), ascorbate peroxidase (APX), and catalase (CAT). SODs act as the first line of defense against ROS. There are three types of SODs in plants based on different metal ligands involved copper/zinc SOD (Cu/Zn-SOD, also known as CSD), manganese SOD (Mn-SOD) and iron SOD (Fe-SOD) (Guan et al., 2013). There are three CSD isozymes which are localized in different cellular compartments in *Arabidopsis*: cytosolic CSD1, chloroplastic CSD2 and peroxisomeic CSD3 (Huang et al., 2011). In *Arabidopsis*, there is a copper chaperone for superoxide dismutase (CCS, which delivers copper to the CSD) to activate all three CSD isozymes activities (Huang et al., 2011). Overexpression of *CSD1* and *CSD2* enhances the tolerance of transgenic plants to UV and high light treatment, salt and heavy metal stresses (Leng et al., 2017; Sunkar et al., 2006). SODs have also been reported to play roles in the hypersensitive response (HR) during cotton-*Xanthomonas campestris* interaction and barley-*Blumeria graminis* interaction (Voloudakis et al., 2006; Xu et al., 2014b).

MicroRNAs (miRNAs) are approximately 21 or 22 nucleotide (nt) long non-coding RNAs that play essential roles in gene silencing by targeting mRNA for cleavage, or by translational repression in both plants and animals (Reinhart et al., 2000; Reinhart et al., 2002). Primary miRNAs (pri-miRNAs) are transcribed by RNA polymerase II but contain an imperfect stem-loop or hairpin structure (Voinnet, 2009; Xie et al., 2015). miRNAs are released from their pri-miRNAs by RNase III-like Dicer-like enzymes in plants (Margis et al., 2006), and then associate with argonaute (AGO) protein (Mallory and Vaucheret, 2010) to inhibit gene expression at transcriptional gene silencing (TGS) or post-transcriptional gene silencing (PTGS) levels (Bologna and Voinnet, 2014). Hundreds of miRNAs have now been discovered through deep-sequencing and genetic approaches (Meyers et al., 2006), and they have been shown to play vital roles in plant development (Couzigou and Combier, 2016; Guo et al., 2017; Huang et al., 2017; Zhang et al., 2017) and responses to biotic and abiotic stresses (Deng et al., 2018; Ding et al., 2017; Kumar, 2014; Li et al., 2017).

Intriguingly, miRNAs are considered as important regulators of R gene expression. For example, two miRNAs, nta-miR6019 and nta-miR6020, were reported to guide the cleavage of the tobacco mosaic virus (TMV) resistance gene, *N*, which is a toll and interleukin-1 receptor-NBS-LRR immune receptor (Li et al., 2012). Furthermore, miR482/2118 is another well-known miRNA that targets the *NBS-LRR* resistance genes (Shivaprasad et al., 2012). Therefore, miRNA-mediated repression of *NBS-LRR* genes is an efficient mechanism for plants to balance the trade-off between growth and defense. The miRNA known specifically as miR398 has been reported to play a role in responses to various abiotic stresses by modulating the expression of its target genes (Zhu et al., 2011; Wang et al., 2016). miR398b was the first miRNA reported to be down-

regulated in response to biotic stress (*P. syringae*) in *Arabidopsis* (Jagadeeswaran et al., 2009; Li et al., 2010). In our previous work, we also found that miR398b plays a role in temperature stress through miRNA and degradome sequencing (Wang et al., 2016). To date, four targets of miR398 have been reported through computational prediction and sequence analysis: *CSD1*, *CSD2*, *CCS* and *COX-5b* (a subunit of the mitochondrial cytochrome c oxidase) in *Arabidopsis* (Beauclair et al., 2010; Jones-Rhoades and Bartel, 2004). Some studies also show that miR398 negatively regulates the PTI response and resistance to pathogenic bacteria (Li et al., 2010). However, whether miR398 can participate in the ETI response and resistance to fungal pathogens *V. dahliae* is not known. Here, we investigated the potential role of miR398b in cotton-*V. dahliae* interaction. The results indicate that miR398b can target both *NBS-LRR* genes and CSD family genes to suppress the resistance of cotton to *V. dahliae*.

RESULTS

Overexpression of miR398b impairs Verticillium wilt resistance in cotton

Expression of miR398b is differentially regulated in cotton in response to *V. dahliae* infection (He et al., 2014; Yin et al., 2012). Therefore, miR398b may be an important regulator in the resistance of cotton to multiple stresses. We first validated the expression patterns of miR398b by reverse transcription quantitative PCR (RT-qPCR) in various cotton tissues. The results revealed that miR398b was expressed in all tissues tested, with highest expression level in the root and anther tissues (Figure 1A). To further verify the expression pattern of miR398b, a 1,233-bp upstream fragment of miR398b was introduced into a construct upstream of the β -glucuronidase (GUS) reporter gene (Jefferson et al., 1987) and transformed into *Arabidopsis* for GUS expression analyses. The GUS staining pattern revealed that expression of miR398b was suppressed in the roots and cotyledons when treated with flg22, nlp20, and *V. dahliae* in *Arabidopsis* (Figure 1B). Analyses of these results indicated that the expression of miR398b was down-regulated upon *V. dahliae* infection in these tissues.

To further understand the function of miR398b in cotton upon *V. dahliae* infection, an miR398b-overexpression vector was prepared and transformed into cotton. Two miR398b-overexpression lines with single copy insertion (O8-17, O8-18) and two null lines (ON and TN) were obtained (Figure S1A). The results of this expression analysis showed that miR398b was highly expressed in miR398b-overexpressing plants (Figure S1C). To test whether the expression level of miR398b affected the resistance of cotton to *V. dahliae*, the transgenic lines were inoculated with *V. dahliae* isolate V592. Compared to the two null lines, the miR398b-overexpressing plants were more susceptible to *V. dahliae* with more obvious wilt symptoms and a higher disease index than the null plants (Figure 2A, B, C). These observations were confirmed by quantification of the DNA levels of *V. dahliae* in the tissues, where the fungal biomass was seven-fold higher in miR398b-overexpressing plants than that in the null plants (Figure 2D). In summary, the results indicate that miR398b suppresses defense in cotton in response to *V. dahliae*.

NBS-LRR genes are targets for miR398b and involved in cotton resistance to *V. dahliae*.

In our previous degradome sequencing data (Wang et al., 2016), two *NBS-LRR* genes (*Gh_A04G0380* and *Gh_D05G3257*) were identified as putative targets of miR398b. *Ghir_D05G34520* and *Ghir_A04G004640* (the corresponding genes of *Gh_D05G3257* and *Gh_A04G0380* in 3rd generation genome data of cotton) contain a CC-NBS-ARC domain and two internal repeat regions. The miR398b target site is localized in the first internal repeat region of *Ghir_D05G34520* (Figure 3A, Figure S2A, B). The expression level of *Gh_D05G3257* was examined, revealing that the transcripts of *Gh_D05G3257* were decreased in miR398b-overexpression lines (Figure 3B). The transcripts of *Gh_D05G3257* were up-regulated in both WT and transgenic plants upon inoculation of pathogen, while the expression levels of *Gh_D05G3257* in transgenic plants were significantly reduced as compared with WT plants (Figure 3B). Also, *Gh_D05G3257* transcripts were highly expressed in roots, hypocotyls, and stems, tissues of which are heavily colonized by *V. dahliae*. The expression levels of *Gh_D05G3257* were significantly up-regulated upon *V. dahliae* infection (Figure S3A, B). Two reads containing the cleavage site were detected in our normalized degradome data, which may suggest that the expression level of *Gh_D05G3257* and *Gh_A04G0380* may not be suppressed through cleavage (Figure 3A). A

plant small RNA target analysis server psRNATarget (Dai et al., 2018) was used to identify the interaction between miR398b and *Gh_D05G3257*, *Gh_A04G0380* genes. Analyses of these results showed that miR398b repressed the expression of *NBS-LRR* genes by translational inhibition (Table S1) and this may be the reason that it is difficult to verify cleavage by 5' random amplification of cDNA ends (RACE).

To confirm the repression activity of miR398b on *NBS-LRR* genes, a luciferase reporter system was employed with about 100 bp-length target sites inserted into the 5' UTR region of the Luciferase (LUC) encoding gene, and a miRNA precursor sequence was cloned into another vector driven by the CaMV35s promoter (Figure 3C). Both constructs were transformed into *Agrobacterium* and infiltrated into *Nicotiana benthamiana* leaves for transient expression assays, where miR157 was used as the negative control and the target site of *GhCSD2* as a positive control. Analyses of these results revealed that the luminescence intensity of 4NB-LUC, 5NB-LUC and CSD2-LUC were decreased when co-expressed with miR398b than when expressed alone or co-expressed with miR157 (Figure 3D). The ratios of LUC activity to control renilla luciferase (RLUC) activity were also detected and showed consistent results in the extracted total protein from the infiltrated sites of the leaf (Figure 3E).

Additionally, the 21 bp target sites of *5NB* (*5NBts*) and the mutated target sites (mts) of *5NB* (*5NBmts*) were fused at the 5'-terminus of *GFP*, respectively (Figure 4A). The *35S:5NBts-GFP* and *35S:5NBmts-GFP* constructs were co-expressed with either the *35S:miR398b* or the *35S:miR157* vector by *Agrobacterium*-mediated transient transformation in tobacco leaves. Analyses of the results revealed that the fluorescence intensity and protein content of *5NBts-GFP* were clearly decreased when co-expressed with miR398b than when expressed alone or co-expressed with miR157. However, *5NBmts-GFP* intensity and protein levels were not influenced when co-expressed with miR398b or miR157 (Figure 4B, C). These results demonstrate that these two *NBS-LRR* genes could be inhibited at the post-transcription level by miR398b.

To further understand the function of the two *NBS-LRR* genes in cotton response to *V. dahliae*, VIGS was employed to knock down the expression levels of both genes. The results revealed that knock-down of *NBS-LRR* genes made the plants more susceptible to *V. dahliae* (Figure 5A). The *TRV:NB-ARC* plants showed severe necrotic vascular bundles with a higher disease indices compared to the *TRV:00* plants (Figure 5B, C). Also, more fungal biomass could be detected in *TRV:NB-ARC* plants inoculated with *V. dahliae* (Figure 5D). We also examined the expression pattern of some defense-related genes in *TRV:NB-ARC* plants upon infection by *V. dahliae*. The results indicate that the expression of genes *GhEDS1*, *GhPAD4*, *GhWRKY28* (genes related to the salicylic acid synthesis and signaling pathway) (Miao et al., 2019) and *GhAOS* (jasmonate acid synthesis-related gene) (Hu et al., 2019) were reduced in *TRV:NB-ARC* plants compared with *TRV:00* plants during *V. dahliae* infection (Figure 5E). These results indicate that knock-down of *NB-ARC* genes reduces cotton resistance to *V. dahliae* by attenuating defense response genes related to SA and JA signal pathways.

miR398b targets *GhCSD* genes and regulates ROS homeostasis

From our previous degradome sequencing data (Wang et al., 2016) and the findings reported in the literature (Beauclair et al., 2010; Sunkar et al., 2006), Cu/Zn SOD family members *CSD1*, *CSD2* and *CCS* were also identified as the target genes of miR398b. To determine whether these family members were similarly regulated in cotton, 5'-RNA ligase-mediated rapid RACE (5'-RLM-RACE) experiments were performed, revealing that *GhCSD1*, *GhCSD2* and *GhCCS* are also targets of miR398b and that their target sites are at the 5'UTR region of *GhCSD1*, the fourth exon of *GhCSD2*, and the last exon of *GhCCS*, respectively (Figure 6A, B, C).

To further understand the function of miR398b and the *GhCSDs* in cotton upon *V. dahliae* infection, the constructs of a miR398b-resistant *GhCSD2* (*GhrCSD2*)-overexpression vector, with six synonymous codon mutations at the miR398b-target sites were prepared (*35S:GhrCSD2*) and transformed into cotton (Figure 6D). Two *GhrCSD2* overexpression lines (T8-14 and T8-15) (Figure S1A and 1B) were obtained. The results of the expression analysis revealed that transcript levels of *GhCSD1*, *GhCSD2* and *GhCCS* were decreased with no difference of *GhCSD3* and *GhCOX-5b* expression levels in miR398b-overexpressing lines (Figure 6E-F).

The transcripts of *GhCSD2* were highly increased in *GhrCSD2*-overexpressing lines (Figure 6E). Expression levels of *GhCSD1*, *GhCSD2* and *GhCCS*, the target genes of miR398b, were up-regulated during pathogen infection (Figure S4A). However, transcript levels of *GhCSD3*, the non-target gene of miR398b, were decreased after *V. dahliae* inoculation (Figure S4A). Furthermore, down-regulation of *GhCSD1*, *GhCSD2*, and *GhCCS* through virus-induced gene silencing (VIGS) rendered the plants more susceptible to *V. dahliae* (Figure S4B, C, D). These results indicate that the members of CSD family, *GhCSD1*, *GhCSD2* and *GhCCS*, as targets of miR398b, are required to mount appropriate defense responses in cotton following challenge with *V. dahliae*.

To investigate the functions of miR398b and *GhCSD* family genes in cotton resistance, we first examined the subcellular location of the CSD family proteins. The results show that GhCSD2, GhCSD3, and GhCCS were localized in the chloroplast, while GhCSD1 exhibited a similar localization pattern as free GFP protein in the cell (Figure S5). Our results showed some differences from the previous study in *Arabidopsis*, whereby AtCSD3 was found to be localized in peroxisomes in *Arabidopsis* (Huang et al., 2011). These results demonstrate that the CSD family members localize in different cellular compartments to regulate ROS homeostasis.

To examine whether redox homeostasis was controlled by miR398b and its *GhCSD* targets in cotton in response to *V. dahliae*, we measured the hydrogen peroxide (H₂O₂) content in cotton roots after Necrosis and ethylene-inducing peptide 1 (Nep1)-like protein 1 (NLP1) treatment. NLP1 are considered as conserved virulence effectors in *V. dahliae* that function as cytolytic toxins. This protein induces plasma membrane leakage, leading to cytotoxicity and necrosis (Ottmann et al., 2009; Qutob et al., 2006). Furthermore, the production of ROS triggered by NLPs induced the onset of lesion formation (Wang et al., 2004). To validate the role of ROS in cotton response to *V. dahliae*, *VdNLP1* was transiently expressed in the cotyledons of miR398b- and *GhrCSD2*-transgenic plants. Necrosis could be observed at the infiltration position 48 h post infiltration (Figure 7A). The results show that overexpression of *GhrCSD2* attenuated necrosis occurs in the presence of NLP1, while overexpression of miR398b resulted in accelerated and increased necrosis. Overexpression of miR398b produced more ROS after treatment with NLP1 (Figure 7B). Together, these results demonstrate that miR398b plays an essential role in regulating ROS homeostasis by targeting CSD family genes, and overexpression of miR398b impairs the ability of ROS scavenging and benefits the invasion of *V. dahliae*.

DISCUSSION

Previously we identified differentially expressed miRNAs including miR8746, miR482, and miR398b, which were putatively involved in targeting *NBS-LRR* disease resistance transcripts (Wang et al., 2016). In this current study, we demonstrated that overexpressing miR398b made plants more susceptible to *V. dahliae* in cotton (Figure 2). In support of these finds, miR398 has been reported to negatively regulate MAMP-triggered immunity (Li et al., 2010) and the expression levels of miR398 were down-regulated upon inoculation of plants with incompatible strains DC3000 (*avrRpm1*) and DC3000 (*avrRpt2*), but not the compatible strain DC3000 (Jagadeeswaran et al., 2009). This implicates involvement of miR398 in both MTI and ETI. In our study, we found that miR398b can target two *NBS-LRR* genes (*Gh_D05G3257* and *Gh_A04G0380*) and the target site of the genes is in the internal region, a region not completely conserved in *NBS-LRR* genes. No identical target sequences were found in the homologous genes in *Oryza sativa*, *Arabidopsis thaliana*, *Zea mays*, *Populus trichocarpa* and *Theobroma cacao*. *Gh_D05G3257* and *Gh_A04G0380* may be unique target genes of miR398b at the post-transcriptional level and contribute to cotton resistance against *V. dahliae* (Figure 3, Figure 4, Figure 5, Table S1). To our knowledge, this is the first report that miR398b can target plant *NBS-LRR* genes to regulate defense responses to a pathogen.

ROS is a general term for oxygen-derived metabolic intermediates or radicals including superoxide (O₂[?]), hydrogen peroxide (H₂O₂), hydroxyl radical (OH[?]) and singlet oxygen (1O₂) (Apel and Hirt, 2004). ROS-generation and -scavenging pathways play an important role both in pathogen virulence and resistance by the host. The ROS burst is reported to be essential for penetration peg formation by *V. dahliae*, and therefore is indispensable for virulence and colonization by this fungus (Zhao et al., 2016). Moreover, excess

ROS produced during plant-pathogen interactions facilitates plant infection and colonization by necrotrophic pathogens (Chung, 2012; Govrin and Levine, 2000). In the host, rapid ROS accumulation also occurs during the cotton-*V. dahliae* interaction but it is quickly scavenged to maintain homeostasis. Thioredoxin GbNRX1, an important apoplastic ROS-scavenger, plays a positive role in the cotton response to *V. dahliae* (Li et al., 2016) and silencing of anthocyanidin synthase (*GbANS*) in cotton increased H₂O₂ production and cell death around the invasion sites, which in turn leads to increased *V. dahliae* infection (Long et al., 2018). These results indicate that ROS elimination after the initial burst may be functionally important in cotton resistance to *V. dahliae*.

Among other players involved in ROS metabolism, superoxide dismutases (SODs) are found in all kingdoms of life and act as the first line of defense against ROS, dismutating superoxide to H₂O₂ (Miller, 2012). In this study, we found that overexpression of miR398b boosted more H₂O₂ production when treated with NLP1 and *V. dahliae* and therefore accelerates the NLP1-triggered cell necrosis (Figure 7). By contrast, overexpression of *GhrCSD2*, which is resistant to miR398b, decreased H₂O₂ content (Figure 7B). These results were strikingly similar to those of recent reports from analyses of rice upon *Magnaporthe oryzae* infection (Li et al., 2019). Additionally, expression levels of *GhMSD1*, *GhFSD2* and *GhRbohB* (the gene putatively encoding NADPH oxidase to catalyze the production of O₂^{[2]-}) were decreased in *GhrCSD2*-overexpression lines upon NLP treatment, but increased in miR398b-overexpression lines compared to WT plants. Meanwhile, transcripts of *GhCSD1*, *GhCCS* and *Gh_D05G3257* (the other target genes of miR398b) were increased in *GhrCSD2*-overexpression lines and decreased in miR398b-overexpression lines (Figure S6). These results suggest that a compensatory regulation mechanism may also exist in cotton ROS homeostasis. However, the phenotypes of miR398- and *GhrCSD2*-overexpression plants in cotton upon pathogen were differ from those in rice. Overexpression of miR398b in cotton impaired cotton resistance to *V. dahliae*, while overexpression of miR398b in rice enhanced resistance to *M. oryzae* (Li et al., 2019). We propose that the excessive ROS accumulation in miR398b-overexpressing plants may damage the cell and facilitate *V. dahliae* infection (Figure 7), consistent with results of previous studies (Chung, 2012; Li et al., 2016).

Taken together, these results suggest that miR398b may function in one of two different ways to regulate plant immunity. First, the results indicate involvement of miR398b in ROS homeostasis through cleaving *GhCSD1*, *GhCSD2* and *GhCCS1*, and second, miR398b suppresses the translation of *NBS-LRR* genes to control defense response (Figure S7). An in-depth account of how miR398b expression is regulated during cotton-*V. dahliae* interactions will be an interesting topic for a future study.

EXPERIMENTAL PROCEDURES

Plant materials and *V. dahliae* proliferation

Seedlings of *G. hirsutum* cv. YZ1, *G. barbadense* cv. 7124 and transgenic lines derived from *G. hirsutum* cv. J668 were grown in a controlled environment chamber under a 16 h light/8 h dark cycle at 25°C for treatment and sampling. *V. dahliae* strain V991 was cultured on Potato Dextrose Agar (PDA) medium for 3~4 days, and hyphae were transferred into Czapek's medium for 3 days at 25°C to prepare suspension solutions.

Infection of cotton seedlings and sample collection

Two-week-old seedlings of *G. barbadense* cv. 7124 and *G. hirsutum* cv. YZ1 were infected with *V. dahliae* conidial suspensions (1×10⁶ conidia·ml⁻¹) using a root dip inoculation method, and control plants were mock-inoculated with sterile water. Roots were harvested at 0 h, 6 h, 12 h, 24 h and 48 h post inoculation, frozen in liquid nitrogen and stored at -80°C for subsequent RNA extraction.

Reverse transcription quantitative-PCR (RT-qPCR) analysis

Stem-loop RT-PCR was used to quantify miRNAs and target genes according to a previous study (Liu et al., 2014). Briefly, 3 µg RNA was reverse-transcribed to cDNA by using stem-loop primers and SuperScript III RT (Invitrogen). The reaction procedure was the following steps: 16°C for 30 min; 60 cycles of 30°C for 30 s, 42°C for 30 s; and then 70°C for 5 min to inactivate the reverse transcriptase.

RT-qPCR was performed using the ABI Prism 7500 system (Applied Biosystems, Foster City, CA, USA) following the manufacturer's protocol. The thermocycling program was as follows: 95°C for 1 min; 40 cycles of 95°C for 10 s, 60°C for 40 s.

RLM-RACE analysis

The 5' RACE procedures were performed using a GeneRacer™ Kit (Invitrogen, <https://www.lifetechnologies.com>). Five micrograms of total RNA from an equal mixture of *G. hirsutum* V991-inoculated samples and *G. barbadense* V991-inoculated samples were ligated to an RNA adapter and reverse-transcribed into cDNA using the GeneRacer Oligo-dT primer. The 5' adaptor primers and 3' gene-specific primers (Table S2) were used to amplify cDNA ends according to the manufacturer's instructions.

Plasmid construction and genetic transformation

To study the expression patterns of miR398b, a 1233 bp promoter region of miR398b was cloned into the pGWB433 vector and used to drive expression of the *GUS* reporter gene in *Arabidopsis*. To localize the CSD family proteins, cDNA sequences lacking stop codons corresponding to *GhCSD1*, *GhCSD2*, *GhCCS* and *GhCSD3* were inserted into the N-terminal GFP-fusion expression vector PMDC84 (Curtis and Grossniklaus, 2003) by Gateway Cloning (Invitrogen, USA). To express VdNLP1:GFP protein, the cDNA sequence of *VdNLP1* lacking the stop codon was inserted into the N-terminal GFP-fusion expression vector PMDC84 by Gateway Cloning. To examine whether miR398b represses the expression of the *NBS-LRR* gene, the 35S promoter with duplicated enhancers was cloned into the reporter vector pGreenII 0800-LUC to generate the vector pGreenII 0800-35s:*LUC*. A 100 bp fragment of *Gh_A04G0380* and *Gh_D05G3257* containing the predicted binding sites was amplified from cotton genomic DNA and ligated into pGreenII 0800-35s:*LUC* at the *Not* I site. The 21 bp target sites of *Gh_D05G3257*(5NBts) and the mutated target sites of *Gh_D05G3257*(5NBmts) were amplified using the primers 5NBts-F/R and 5NBmts-F/R, respectively, according to the method described previously (Li et al., 2019). The isolated fragments were ligated into the N-terminal GFP-fusion expression vector *pMDC84-35s:GFP* at the *Kpn* I site. For VIGS vector construction, fragments of *GhCSD1*, *GhCSD2*, *GhCCS*, and *NB-ARC* were amplified from root samples of *G. hirsutum*. PCR products were digested by two restriction endonucleases, *Bam* HI and *Kpn* I, and ligated to the TRV vector as reported previously (Gao et al., 2013). To study the function of miR398b, a 313 bp genomic sequence containing the miR398b precursor was cloned and ligated into a pK2GW7.0 vector to overexpress the miR398b precursor. The miR157 overexpression vector was generated previously (Liu et al., 2017). A miR398b-resistant version of *GhCSD2* (*rGhCSD2*) was generated by introducing six mutations into the target sites of *GhCSD2* through recombinant PCR and cloned into the vector pK2GW7.0. The primer sequences used in vector construction are listed in Table S2. All vectors were transferred to *Agrobacterium tumefaciens* (GV3101).

For genetic transformation, *Agrobacterium tumefaciens* (strain GV3101)-mediated transformation was used to transform hypocotyl sections of *G. hirsutum* cv. J668 according to a previously described method (Jin et al., 2006). Null plants containing no transgenes were separated from self-pollinated *35s:rCSD2* hemizygotes TN and self-pollinated *35s:miR398b* hemizygotes ON.

Subcellular localization analysis

Agrobacterium tumefaciens strain GV3101 containing binary vectors with the GFP fusion protein were infiltrated into tobacco leaf epidermal cells for transient expression analysis, and the transfected cells were imaged by confocal laser scanning microscopy at 60 h after inoculation, according to Gao et al. (2016). The GFP was excited at a wavelength of 488 nm, and fluorescence emission was collected from 505 to 530 nm. Chlorophyll autofluorescence was excited at a wavelength of 488 nm and collected from 647 to 745 nm.

Virus-induced gene silencing and pathogen inoculation

Agrobacterium tumefaciens cells harboring TRV vectors were infiltrated into two fully expanded cotyledons of 10-day-old seedlings as described previously (Gao et al., 2013). The primers listed in Table S2 were used

to evaluate the silencing effect based on the expression levels of the target genes in leaf and root tissues.

For pathogen inoculation, 3-week-old cotton seedlings of transgenic and VIGS plants (at least 30 plants for each lines) were infected with *V. dahliae* (V991) conidial suspension (1×10^5 conidia·ml⁻¹) using a root dip inoculation method, and the plants were transplanted into sterilized soil for observation of disease symptoms. A fungal recovery assay and a disease index analysis were performed as described previously (Xu et al., 2014a). For fungal colonization and biomass detection, longitudinal cross-sections of cotyledonary nodes were dissected at 16 days after inoculation and observed under a stereoscopic microscope (MZFLIII, Leica, Wetzlar, Germany). Infected stem samples were separately collected for DNA extraction and taken approximately 1 cm above the cotyledon node (CN) and first leaf node (FN). Each experiment was repeated three times.

Expression of VdNLP1 in transgenic cotton plants

Agrobacterium tumefaciens strain GV3101 containing binary vector (PMDC84) encoding the VdNLP1-GFP fusion protein, or the empty vector, was infiltrated into two fully expanded cotyledons of 10-day-old transgenic and wild-type cotton plants. Lesion formation or wilting symptoms were photographed at 48 h post infiltration.

Histochemical assay

Ten-day-old transgenic *Arabidopsis* plants were spread with *V. dahliae* conidial suspension (1×10^6 conidia·ml⁻¹), 2 μ M peptides of either flg22 or nlp20, for 12 h. Peptides of flg22 and nlp20 were synthesized in GenScript (Nanjing, China). Plants were incubated in the GUS staining solution at 37°C for 6 h, followed by decolorization in 75% alcohol and then photographed under stereoscopic microscopy (MZFLIII, Leica, Wetzlar, Germany) according to Sun et al. (2014).

Detection and measurement of ROS

The quantification of H₂O₂ in *V. dahliae*-infected roots of *G. barbadense*, *G. hirsutum*, and leaves of transgenic cotton plants was performed with a commercial H₂O₂ detection kit (Sangon Biotech, Shanghai, China).

Luciferase reporter assay

One hundred microliters of the *Agrobacterium* strain GV3101 containing the *pGreenII 0800-target site-LUC* plasmid were combined with 900 μ l of the *Agrobacterium* strain GV3101 containing either the *35s:pri-miR398b* or *35s:primiR157* plasmid. The mixture was incubated (28°C, 200 rpm, shaker) to a final concentration (OD600 = 1.0), and resuspended in infiltration buffer (10 mM MES, pH 5.6, 10 mM MgCl₂ and 150 μ M acetosyringone) as described previously (Hellens et al., 2005). The same volume of mixed suspensions were injected into leaves of *Nicotiana benthamiana* by agro-infiltration. After 48 h, LUC luminescence was examined using a cryogenically cooled CCD camera (Lumazome PyLoN 2048B) as described previously (Chen et al., 2008). LUC and RLUC activities were measured as counts per second using a multimode plate reader (PerkinElmer) using the Promega kit (N1630).

Green fluorescence protein (GFP) reporter assay

The *A. tumefaciens* strain GV3101 containing one of the binary vector (*35s:5NBts-GFP* or *35s:5NBmts-GFP*, *35s: miR398b*, *35s:miR157*) was cultured in LB medium overnight at 28°C. The *A. tumefaciens* samples with different vectors were collected and mixed at the indicated optical density (O.D.) using a DU800 spectrophotometer (Beckman Coulter). The *A. tumefaciens* harboring different vectors were infiltrated into tobacco leaves and the transfected cells were imaged by confocal laser scanning microscopy (Olympus FV1200) 60 h after inoculation. For western blot analysis, 100 mg of infiltrated leaf tissues was grounded into fine powder in liquid nitrogen and homogenized in 400 μ l of tobacco protein extraction buffer (25 mM Tris-HCl, PH=7.5; 150 mM NaCl; 1 mM EDTA; 0.5% Triton X-100; 5% glycerol; 1% protein inhibitor; 2 mM phenylmethanesulfonyl fluoride). The same amount of extracted total protein was separated on a 15% SDS-PAGE gel, and transferred to a polyvinylidene fluoride membrane (Millipore). A 10,000-fold-diluted

Rabbit Anti-GFP sera (Ab290, Abcam) and Secondary-Goat Anti-Rabbit IgG H&L (HRP) (Ab205718, Abcam) were used to detect GFP accumulation and total protein was stained with Coomassie brilliant blue (R250) for a loading control.

ACCESSION NUMBERS

Sequence data from this article can be found in the CottonGen database (<http://www.cottongen.org>) or GenBank databases under the following accession numbers: *GhCSD1* , Gh_D13G1747; *GhCSD2* , Gh_D09G0858; *GhCSD3* , Gh_D11G2412; *GhCCS* , Gh_D08G1899; *5NB* , Gh_D05G3257; *4NB* , Gh_A04G0380; *GhUB7* , Gh_A11G0969.

AUTHOR CONTRIBUTIONS

L.Z. and X.Z. designed the experiment. Y.M. performed most of the research and drafted the manuscript. J.D., M.S., L.Z., X.N. and C.Y. helped perform the experiments. S.J.K. made comments to the experiments. Y.M. analyzed the data. X.Z., S.J.K., and L.Z revised the manuscript.

Financial sources: Funding support from the National Key Research and Development Program of China (2018YFD0100403) and the project from Ministry of Science and Technology of China (KY201702009) are appreciated.

CONFLICT OF INTEREST

The authors declare no conflict of interest.

ACKNOWLEDGMENTS

The vectors used for VIGS were kindly provided by Prof. Bart Thomma (Laboratory of Phytopathology, Wageningen University and Research Center, The Netherlands). We are grateful to Prof. Guiliang Jian (Institute of Plant Protection, Chinese Academy of Agricultural Sciences, China) for providing *V. dahliae* strain ‘V991’. We would like to thank De Zhu (National key laboratory of crop genetic improvement, Huazhong Agricultural University, Wuhan) for assistance with laser scanning confocal microscopy.

SUPPORTING INFORMATION

Table S1. Model of miR398 repression of the expression of *NBS-LRR* and *CSD* genes by inhibiting translation and mRNA cleavage, respectively. The predictions were accomplished using the plant small RNA target analysis server psRNATarget (<http://plantgrn.noble.org/psRNATarget/>). UPE: unpaired energy required to open secondary structure around miRNA’s target site on mRNA; Less energy represents higher possibility to be an effective target site.

Table S2. Primers used in this study. The primers used for reverse transcription-quantitative PCR (RT-qPCR) and qPCR are marked by ‘RL’; the primers for gateway vector construction are marked by ‘attb’.

Figure S1: Southern blot and transgene expression analysis in cotton.

A: Southern blot analysis of transgenic plants. The single band from each lane represents the single T-DNA insertion of each transgenic line.

B and C: Reverse transcription-quantitative PCR analysis of *GhCSD2* and miR398b expression levels in miR398b-resistant *GhCSD2* overexpressing (OEGhrCSD2) transgenic plants and miR398b-overexpressing transgenic plants, respectively. Values represent the means \pm s. d. from three biological replicates.

Figure S2: Comparison of amino acid sequences of nucleotide binding site regions 4NB and 5NB in cotton proteins Ghir_A04G004640 and Ghir_D05G34520.

A: Comparison of amino acid sequences for *Ghir_A04G004640* (4NB) and *Ghir_D05G34520* (5NB), the target site is marked by red box.

B: Gene structure of *Ghir_D05G34520* (5NB), the conserved domains are predicted by SMART. The target region of miR398b is indicated by red box and is in the first internal repeat region of 5NB.

Figure S3: Tissue-specific and *Verticillium dahliae*-induced expression patterns of the cotton 5NB gene.

A: Reverse transcription-quantitative PCR (RT-qPCR) analysis of expression levels of the 5NB gene in cotton root, hypocotyl, stem, leaf, ovule and fiber. Values represent means \pm s. d. from three biological replicates.

B: RT-qPCR analysis of 5NB gene responses to *V. dahliae* infection. Values represent the means \pm s. d. from three biological replicates.

Figure S4: GhCSD family members positively regulate cotton resistance to *Verticillium dahliae*.

A: Reverse transcription-quantitative PCR (RT-qPCR) evaluation of the relative expression levels of *GhCSD1*, *GhCSD2*, *GhCSD3* and *GhCCS* induced by *V. dahliae* at different time points, as compared with mock treatment. Values represent the means \pm s. d. from three biological replicates.

B: Disease symptoms of cotton transformed with various *TRV* constructs: *TRV:00*, *TRV:GhCSD1*, *TRV:GhCSD2*, *TRV:GhCCS*, *TRV:NB-ARC* plants 16 days after inoculation with ‘V991’. Photos were obtained 16 days after inoculation.

C: Relative expression levels of the corresponding genes in root samples from *TRV:00* and *TRV:target-genes* plants RT-qPCR.

D: Disease index statistics of *TRV:00* and *TRV:target-genes* plants at 16 days after inoculation.

Figure S5: Sub-cellular localization and *Verticillium dahliae*-induced expression patterns of *GhCSD1*, *GhCSD2*, *GhCSD3*, and *GhCCS*. Transient expression of green fluorescent protein (GFP) or the GhCSD1-GFP, GhCSD2-GFP, GhCSD3-GFP, GhCCS-GFP fusion proteins in tobacco leaf cells. The green color indicates GFP expression, and red color indicates chloroplast autofluorescence, Bars= 20 μ m.

Figure S6: Overexpression of miR398b and *GhrCSD2* affect the expression levels of other SOD members in cotton upon NLP treatments. Reverse transcription-quantitative qPCR (RT-qPCR) analysis showing the relative expression patterns of *GhMSD1*, *GhFSD2*, *GhCSD1*, *GhCCS*, *GhRbohB*, and *5NB* in wild-type (WT) and transgenic plants upon NLP treatment.

Figure S7: Co-expression networks of the miR398b target modules in cotton. Diagram was drawn using ccNET (structural biology.cau.edu.cn). Gh_D09G0858, Gh_D05G3257 and Gh_A04G0380 are cotton gene IDs for *GhCSD2*, *5NB* and *4NB*, respectively.

FIGURE LEGENDS

Figure 1: Expression patterns of the cotton microRNA miR398b in different tissues and in defense responses.

A: Reverse transcription-quantitative PCR analysis for expression levels of miR398b in different tissues. R: root; S: stem; L: leaf; P: petal; A: anther; 0 d: 0 d ovule; 5 d: 5 d fiber after flowering. The expression levels of miR398b were normalized to *GhUB7*. The bar represents the standard error from three biological repeats and the lowercase letter above the column represents significant difference by statistical analysis using the linear mode method, completely randomized AOV, and all-pairwise comparisons (LSD, 0.05).

B: Histochemical β -glucuronidase (GUS) staining analysis of the expression patterns of pmiR398b::GUS in two independent lines of transgenic *Arabidopsis* leaves and roots after subjected to 12 h for flg22, nlp20, and *Verticillium dahliae* treatments. Bars = 200 μ m.

Figure 2: Overexpression of miR398b attenuates cotton resistance to *Verticillium dahliae*.

A: Verticillium wilt disease symptoms of null cotton plants (ON and TN) and miR398b overexpressing lines (O8-17 and O8-18) at 16 days post-inoculation with *V. dahliae*.

B: Dark, necrotic vascular bundles of the dissected stems of each line were photographed 16 days after *V. dahliae* inoculation. Fluorescence imaging shows V592-GFP hyphae in the vascular bundles of miR398b overexpression lines.

C: Disease index statistics of null plants (ON and TN) and miR398b overexpressing lines (O8-17 and O8-18) at 16 d after inoculation. The bar represents the standard error from three biological repeats and the lowercase above the column represent the significance by statistical analysis using the linear mode method, completely randomized AOV, and all-pairwise comparisons (LSD, 0.05).

D: PCR quantification of fungal biomass. The biomass represents the levels of amplification of the *Verticillium* internal transcribed spacer (ITS) region compared to the levels of cotton *GhUB7* amplification. Values represent the means \pm s. d. from three biological replicates (** P<0.01, Student's t-test).

Figure 3: The cotton microRNA miR398b inhibits the expression of *NBS-LRR* defense signaling associated genes.

A: Schematic diagram of 4*NB* and 5*NB* target sites of miR398b validated through degradome sequencing.

B: RT-qPCR analysis of expression levels of *NBS-LRR* genes in root samples of miR398b overexpressing lines and in root samples of wild type plants and miR398b overexpressing lines inoculated with *Verticillium dahliae*. The bar represents the standard error from three biological repeats and the lowercase above the column represent the significance by statistical analysis using the linear mode method, completely randomized AOV, and all-pairwise comparisons (LSD, 0.05).

C: Schematics of dual-luciferase system containing 4*NB*, 5*NB* target sites in the 5'UTR region of the luciferase (LUC) gene, respectively.

D: Inhibition of the expression of *NBS-LRR* genes by miR398b. Agrobacterium-mediated transient expression of the 4*NB*-LUC and 5*NB*-LUC fusion proteins with miR398b and miR157 in tobacco leaf cells with *Agrobacterium tumefaciens* cultures grown to the same optical density. After 48 h, LUC luminescence was examined using a cryogenically cooled CCD camera (Lumazome PyLoN 2048B)

E: Quantification of LUC/RLUC intensity and miR398b mRNA levels. Values represent the means \pm s. d. from three biological replicates (* P value [?] 0.05, ** P value [?] 0.01, Student's t-test).

Figure 4: MicroRNA miR398b suppresses the expression of *NBS-LRR* defense signaling gene in cotton.

A: Schematics of 5*NB*ts (5*NB* target sites)-green fluorescent protein (GFP) and 5*NB*mts (5*NB*-mutated target sites)-GFP fusion proteins and alignment sequences of 5*NB*ts and 5*NB*mts with miR398b and miR157, respectively. Bases in red indicate the mutated nucleotides.

B: GFP fluorescence shows that miR398b represses the expression of 5*NB*. *Agrobacterium tumefaciens* mediated transient expression of 5*NB*ts-GFP and 5*NB*mts-GFP fusion proteins with miR398b and miR157 in tobacco leaf cells at the indicated optical densities (O.D.). Laser confocal microscopy was used to observe the green fluorescence 60 h after infiltration by *A. tumefaciens*. * indicated the injection site, Bars=100 μ m.

C: Western blot analysis with an anti-GFP antibody reveals the expression levels of 5*NB*ts-GFP and 5*NB*mts-GFP proteins following each treatment. The total protein was stained with Coomassie brilliant blue as a

loading control.

Figure 5: Suppression of cotton *NBS-LRR* genes increases susceptibility to *Verticillium dahliae*.

A: Disease symptoms of the *TRV:00* and *TRV:NB-ARC* plants following inoculation with isolate V991 of *V. dahliae*. The images were obtained at 16 days post-inoculation (dpi).

B: Dark and necrotic vascular bundles of the dissected stems from *TRV:00* and *TRV:NB-ARC* plants at 16 dpi with *V. dahliae*.

C: Disease index statistics of *TRV:00*, *TRV:NB-ARC* plants from 12 d to 15 dpi with *V. dahliae*.

D: Fungal biomass determined by quantitative PCR in *TRV:00* and *TRV:NB-ARC* cotton plants. The relative biomass is represented by the DNA quantification levels of *Verticillium* Internal Transcribed Spacer (ITS) compared to the of cotton *UB7*. CN = samples from the cotyledonary nodes of cotton stems; FN = samples from the first internode. Values represent the means \pm s. d. from three biological replicates (** P value [?] 0.01, Student's t-test).

E: Suppression of cotton *NBS-LRR* genes attenuates the expression of defense-related genes upon *V. dahliae* infection. Values represent the means \pm s. d. from three biological replicates.

Figure 6: The microRNA miR398b can guide the cleavage of *GhCSD1*, *GhCSD2* and *GhCCS* in cotton.

A: Schematic diagram of *GhCSD2* target site for miR398b, validated through degradome sequencing and RNA ligase-mediated rapid random amplification of cDNA ends (RLM-RACE). Watson-Crick pairing (vertical dashes) and non-Watson-Crick pairing (colon) are indicated. The number of miR398b cleavage products is indicated with bold font and arrow.

B-C: Schematic diagram of *GhCSD1* (**B**) and *GhCCS* (**C**) target sites of miR398b determined by RLM-RACE experiments.

D: Schematic representation of miR398b-resistant *GhCSD2* (*rCSD2*) vector constructed by synonymous mutation. The top strand depicts the original miR398b target site of *GhCSD2* from 421 to 441 nt calculated from the start codon, and the bottom strand shows the sequence post-mutation; bases in red indicate the nucleotides that were replaced.

E-F: Reverse transcription-quantitative PCR analysis of the expression of miR398b, the target genes *GhCSD2*, *GhCSD1*, *GhCCS*, and the non-target genes *GhCSD3* and *GhCOX-5b* in roots of wild type, null, miR398b-overexpressing (O8-15, O8-17, O8-18, O8-41) and miR398b-resistant *GhCSD2* overexpressing (T8-14, T8-15) lines. Bars represent means and standard error of three technical replicates.

Figure 7: Overexpression of miR398b in cotton results in constitutive reactive oxygen species (ROS) accumulation and defective ROS elimination in response to *Verticillium dahliae*.

A: Necrotic lesions on treated cotyledons of wild type and transgenic plants. Images were obtained 48 h post leaf infiltration of the necrosis and ethylene-inducing peptide 1-like protein 1 (NLP1) expressed via *Agrobacterium tumefaciens*-mediated plant transformation. The gel picture shows the expression analysis of *NLP1* in cotton cotyledons by RT-PCR (e: empty vector; N: NLP1).

B: ROS quantification in NLP1-treated cotyledons of wild type and transgenic cotton. The bar represents the standard error from three biological repeats and the lowercase letter above the respective columns represents the statistical significance of as determined using the linear mode method, completely randomized AOV, and all-pairwise comparisons (LSD, 0.05).

REFERENCES

Apel, K. and Hirt, H. (2004) Reactive oxygen species: metabolism, oxidative stress, and signal transduction. *Annu Rev Plant Biol* **55**, 373-399.

Beauclair, L., Yu, A. and Bouche, N. (2010) microRNA-directed cleavage and translational repression of the copper chaperone for superoxide dismutase mRNA in *Arabidopsis*. *Plant J* **62**, 454-462.

Bologna, N.G. and Voinnet, O. (2014) The diversity, biogenesis, and activities of endogenous silencing small RNAs in *Arabidopsis*. *Annu Rev Plant Biol* **65**, 473-503.

Chen, H., Zou, Y., Shang, Y., Lin, H., Wang, Y., Cai, R., Tang, X. and Zhou, J.M. (2008) Firefly luciferase complementation imaging assay for protein-protein interactions in plants. *Plant physiol* **146**, 368-376.

Chisholm, S.T., Coaker, G., Day, B. and Staskawicz, B.J. (2006) Host-microbe interactions: shaping the evolution of the plant immune response. *Cell* **124**, 803-814.

Chung, K.R. (2012) Stress response and pathogenicity of the necrotrophic fungal pathogen *Alternaria alternata*. *Scientifica* **2012**, 635431.

Couzigou, J.M. and Combier, J.P. (2016) Plant microRNAs: key regulators of root architecture and biotic interactions. *New phytol* **212**, 22-35.

Curtis, M.D. and Grossniklaus, U. (2003) A gateway cloning vector set for high-throughput functional analysis of genes in planta. *Plant physiol* **133**, 462-469.

Dai, X., Zhuang, Z. and Zhao, P.X. (2018) psRNATarget: a plant small RNA target analysis server (2017 release). *Nucleic acids research* **46**, W49-W54.

Deng, Y., Wang, J., Tung, J., Liu, D., Zhou, Y., He, S., Du, Y., Baker, B. and Li, F. (2018) A role for small RNA in regulating innate immunity during plant growth. *PLoS pathog* **14**, e1006756.

Ding, Y., Ma, Y., Liu, N., Xu, J., Hu, Q., Li, Y., Wu, Y., Xie, S., Zhu, L., Min, L. and Zhang, X. (2017) microRNAs involved in auxin signalling modulate male sterility under high-temperature stress in cotton (*Gossypium hirsutum*). *Plant J* **91**, 977-994.

Gao, W., Long, L., Xu, L., Lindsey, K., Zhang, X. and Zhu, L. (2016) Suppression of the homeobox gene HDTF1 enhances resistance to *Verticillium dahliae* and *Botrytis cinerea* in cotton. *J Integr Plant Biol* **58**, 503-513.

Gao, W., Long, L., Zhu, L., Xu, L., Gao, W., Sun, L., Liu, L. and Zhang, X. (2013) Proteomic and virus-induced gene silencing (VIGS) analyses reveal that gossypol, brassinosteroids, and jasmonic acid contribute to the resistance of cotton to *Verticillium dahliae*. *Mol Cell Proteomics* **12**, 3690-3703.

Govrin, E.M. and Levine, A. (2000) The hypersensitive response facilitates plant infection by the necrotrophic pathogen *Botrytis cinerea*. *Curr Biol* **10**, 751-757.

Guan, Q., Lu, X., Zeng, H., Zhang, Y. and Zhu, J. (2013) Heat stress induction of miR398 triggers a regulatory loop that is critical for thermotolerance in *Arabidopsis*. *Plant J* **74**, 840-851.

Guo, C., Xu, Y., Shi, M., Lai, Y., Wu, X., Wang, H., Zhu, Z., Poethig, R.S. and Wu, G. (2017) Repression of miR156 by miR159 regulates the timing of the juvenile-to-adult transition in *Arabidopsis*. *Plant cell* **29**, 1293.

He, X., Sun, Q., Jiang, H., Zhu, X., Mo, J., Long, L., Xiang, L., Xie, Y., Shi, Y., Yuan, Y. and Cai, Y. (2014) Identification of novel microRNAs in the *Verticillium* wilt-resistant upland cotton variety KV-1 by high-throughput sequencing. *SpringerPlus* **3**, 564.

Hellens, R.P., Allan, A.C., Friel, E.N., Bolitho, K., Grafton, K., Templeton, M.D., Karunairetnam, S., Gleave, A.P. and Laing, W.A. (2005) Transient expression vectors for functional genomics, quantification of promoter activity and RNA silencing in plants. *Plant methods* **1**, 13.

Hu, Q., Zhu, L.F., Zhang, X.N., Guan, Q.Q., Xiao, S.H., Min, L., Zhang, X.L. (2018) GhCPK33 negatively regulates defense against *Verticillium dahliae* by phosphorylating GhOPR3. *Plant Physiol* **178**, 876-889.

Huang, C.H., Kuo, W.Y., Weiss, C. and Jinn, T.L. (2011) Copper chaperone-dependent and -independent activation of three copper-zinc superoxide dismutase homologs localized in different cellular compartments in *Arabidopsis*. *Plant physiol* **158**, 737-746.

Huang, W., Peng, S., Xian, Z., Lin, D., Hu, G., Yang, L., Ren, M. and Li, Z. (2017) Overexpression of a tomato miR171 target gene SlGRAS24 impacts multiple agronomical traits via regulating gibberellin and auxin homeostasis. *Plant biotechnol J* **15**, 472-488.

Jagadeeswaran, G., Saini, A. and Sunkar, R. (2009) Biotic and abiotic stress down-regulate miR398 expression in *Arabidopsis*. *Planta* **229**, 1009-1014.

Jefferson, R.A., Kavanagh, T.A., Bevan, M.W. (1987) GUS fusions: beta-glucuronidase as a sensitive and versatile gene fusion marker in higher plants. *EMBO J* **6**, 3901-3907

Jin, S., Zhang, X., Nie, Y., Guo, X., Liang, S. and Zhu, H. (2006) Identification of a novel elite genotype for in vitro culture and genetic transformation of cotton. *Biol Plant* **50**, 519-524.

Jones-Rhoades, M.W. and Bartel, D.P. (2004) Computational identification of plant microRNAs and their targets, including a stress-induced miRNA. *Mol cell* **14**, 787-799.

Jones, J.D. and Dangl, J.L. (2006) The plant immune system. *Nature* **444**, 323-329.

Klosterman, S.J., Atallah, Z., Vallad, G.E., Subbarao, K.V. (2009) Diversity, pathogenicity, and management of *Verticillium* species. *Annu Rev Phytopathol* **47**, 39-62.

Kumar, R. (2014) Role of microRNAs in biotic and abiotic stress responses in crop plants. *Appl Biochem Biotechnol* **174**, 93-115.

Leng, X., Wang, P., Zhu, X., Li, X., Zheng, T., Shangguan, L. and Fang, J. (2017) Ectopic expression of CSD1 and CSD2 targeting genes of miR398 in grapevine is associated with oxidative stress tolerance. *Functional & integrative genomics* **17**, 697-710.

Li, F., Pignatta, D., Bendix, C., Brunkard, J.O., Cohn, M.M., Tung, J., Sun, H., Kumar, P. and Baker, B. (2012) MicroRNA regulation of plant innate immune receptors. *Proc Nat Acad Sci USA* **109**, 1790-1795.

Li, S., Castillo-Gonzalez, C., Yu, B. and Zhang, X. (2017) The functions of plant small RNAs in development and in stress responses. *Plant J* **90**, 654-670.

Li, Y., Cao, X.L., Zhu, Y., Yang, X.M., Zhang, K.N., Xiao, Z.Y., Wang, H., Zhao, J.H., Zhang, L.L., Li, G.B., Zheng, Y.P., Fan, J., Wang, J., Chen, X.Q., Wu, X.J., Zhao, J.Q., Dong, O.X., Chen, X.W., Chern, M. and Wang, W.M. (2019) Osa-miR398b boosts H₂O₂ production and rice blast disease-resistance via multiple superoxide dismutases. *New phytol*.

Li, Y., Zhang, Q., Zhang, J., Wu, L., Qi, Y. and Zhou, J.M. (2010) Identification of microRNAs involved in pathogen-associated molecular pattern-triggered plant innate immunity. *Plant physiol* **152**, 2222-2231.

Li, Y.B., Han, L.B., Wang, H.Y., Zhang, J., Sun, S.T., Feng, D.Q., Yang, C.L., Sun, Y.D., Zhong, N.Q. and Xia, G.X. (2016) The thioredoxin *GbNRX1* plays a crucial role in homeostasis of apoplastic reactive oxygen species in response to *Verticillium dahliae* infection in cotton. *Plant physiol* **170**, 2392-2406.

Liu, N., Tu, L., Tang, W., Gao, W., Lindsey, K. and Zhang, X. (2014) Small RNA and degradome profiling reveals a role for miRNAs and their targets in the developing fibers of *Gossypium barbadense*. *Plant J* **80**, 331-344.

Long, L., Zhao, J.-R., Xu, F.-C., Yang, W.-W., Liao, P., Gao, Y., Gao, W. and Song, C.-P. (2018) Silencing of GbANS reduces cotton resistance to *Verticillium dahliae* through decreased ROS scavenging during the pathogen invasion process. *Plant Cell, Tissue and Organ Culture (PCTOC)* **135**, 213-221.

Mallory, A. and Vaucheret, H. (2010) Form, function, and regulation of ARGONAUTE proteins. *Plant Cell* **22**, 3879-3889.

- Margis, R., Fusaro, A.F., Smith, N.A., Curtin, S.J., Watson, J.M., Finnegan, E.J. and Waterhouse, P.M. (2006) The evolution and diversification of Dicers in plants. *FEBS Lett* **580** , 2442-2450.
- Meyers, B.C., Souret, F.F., Lu, C. and Green, P.J. (2006) Sweating the small stuff: microRNA discovery in plants. *Curr Opin Biotechnol* **17** , 139-146.
- Miao, Y.H., Xu, L., He, X., Zhang, L., Shaban, M., Zhang, X.L., Zhu, L.F. (2019) Suppression of tryptophan synthase activates cotton immunity by triggering cell death via promoting SA synthesis. *Plant J* **98** , 329-345
- Miller, A.F. (2012) Superoxide dismutases: Ancient enzymes and new insights. *FEBS Letters* **586** , 585-595.
- Mittler, R. (2017) ROS are good. *Trends in plant science* **22** , 11-19.
- Mittler, R., Vanderauwera, S., Suzuki, N., Miller, G., Tognetti, V.B., Vandepoele, K., Gollery, M., Shulaev, V. and Van Breusegem, F. (2011) ROS signaling: the new wave? *Trends in plant science* **16** , 300-309.
- Ottmann, C., Luberaeki, B., Kufner, I., Koch, W., Brunner, F., Weyand, M., Mattinen, L., Pirhonen, M., Anderluh, G., Seitz, H.U., Nurnberger, T. and Oecking, C. (2009) A common toxin fold mediates microbial attack and plant defense. *Proc Nat Acad Sci USA* **106** , 10359-10364.
- Qutob, D., Kemmerling, B., Brunner, F., Kufner, I., Engelhardt, S., Gust, A.A., Luberaeki, B., Seitz, H.U., Stahl, D., Rauhut, T., Glawischnig, E., Schween, G., Lacombe, B., Watanabe, N., Lam, E., Schlichting, R., Scheel, D., Nau, K., Dodt, G., Hubert, D., Gijzen, M. and Nurnberger, T. (2006) Phytotoxicity and innate immune responses induced by Nep1-like proteins. *Plant Cell* **18** , 3721-3744.
- Reinhart, B.J., Slack, F.J., Basson, M., Pasquinelli, A.E., Bettinger, J.C., Rougvie, A.E., Horvitz, H.R. and Ruvkun, G. (2000) The 21-nucleotide let-7 RNA regulates developmental timing in *Caenorhabditis elegans* . *Nature* **403** , 901.
- Reinhart, B.J., Weinstein, E.G., Rhoades, M.W., Bartel, B. and Bartel, D.P. (2002) MicroRNAs in plants. *Genes & development* **16** , 1616-1626.
- Shivaprasad, P.V., Chen, H.M., Patel, K., Bond, D.M., Santos, B.A. and Baulcombe, D.C. (2012) A microRNA superfamily regulates nucleotide binding site-leucine-rich repeats and other mRNAs. *Plant Cell* **24** , 859-874.
- Sun, L., Zhu, L., Xu, L., Yuan, D., Min, L. and Zhang, X. (2014) Cotton cytochrome P450 CYP82D regulates systemic cell death by modulating the octadecanoid pathway. *Nat commun* **5** , 5372.
- Sunkar, R., Kapoor, A. and Zhu, J.K. (2006) Posttranscriptional induction of two Cu/Zn superoxide dismutase genes in Arabidopsis is mediated by downregulation of miR398 and important for oxidative stress tolerance. *Plant Cell* **18** , 2051-2065.
- Tian, D., Traw, M.B., Chen, J.Q., Kreitman, M. and Bergelson, J. (2003) Fitness costs of R-gene-mediated resistance in Arabidopsis thaliana. *Nature* **423** , 74.
- van der Biezen, E.A. and Jones, J.D.G. (1998) The NB-ARC domain: a novel signalling motif shared by plant resistance gene products and regulators of cell death in animals. *Curr Biol* **8** , R226-R228.
- Voinnet, O. (2009) Origin, biogenesis, and activity of plant microRNAs. *Cell* **136** , 669-687.
- Voloudakis, A.E., Marmey, P., Delannoy, E., Jalloul, A., Martinez, C. and Nicole, M. (2006) Molecular cloning and characterization of *Gossypium hirsutum* superoxide dismutase genes during cotton–Xanthomonas campestris pv. malvacearum interaction. *Physiol Mol Plant Pathol* **68** , 119-127.
- Wang, J.Y., Cai, Y., Gou, J.Y., Mao, Y.B., Xu, Y.H., Jiang, W.H. and Chen, X.Y. (2004) VdNEP, an elicitor from *Verticillium dahliae* , induces cotton plant wilting. *Appl Environ Microbiol* **70** , 4989-4995.
- Wang, Q., Liu, N., Yang, X., Tu, L. and Zhang, X. (2016) Small RNA-mediated responses to low- and high-temperature stresses in cotton. *Sci Rep* **6** , 35558.

Xie, M., Zhang, S. and Yu, B. (2015) microRNA biogenesis, degradation and activity in plants. *Cell Mol Life Sci* **72** , 87-99.

Xu, L., Zhang, W., He, X., Liu, M., Zhang, K., Shaban, M., Sun, L., Zhu, J., Luo, Y., Yuan, D., Zhang, X. and Zhu, L. (2014a) Functional characterization of cotton genes responsive to *Verticillium dahliae* through bioinformatics and reverse genetics strategies. *J Exp Bot* **65** , 6679-6692.

Xu, L., Zhu, L.-F. and Zhang, X.-L. (2013) Research on resistance mechanism of cotton to *Verticillium wilt*. *Acta Agronomica Sinica* **38** , 1553-1560.

Xu, W., Meng, Y. and Wise, R.P. (2014b) Mla- and Rom1-mediated control of microRNA398 and chloroplast copper/zinc superoxide dismutase regulates cell death in response to the barley powdery mildew fungus. *New phytol* **201** , 1396-1412.

Yin, Z., Li, Y., Han, X. and Shen, F. (2012) Genome-wide profiling of miRNAs and other small non-coding RNAs in the *Verticillium dahliae* -inoculated cotton roots. *PLoS one* **7** , e35765.

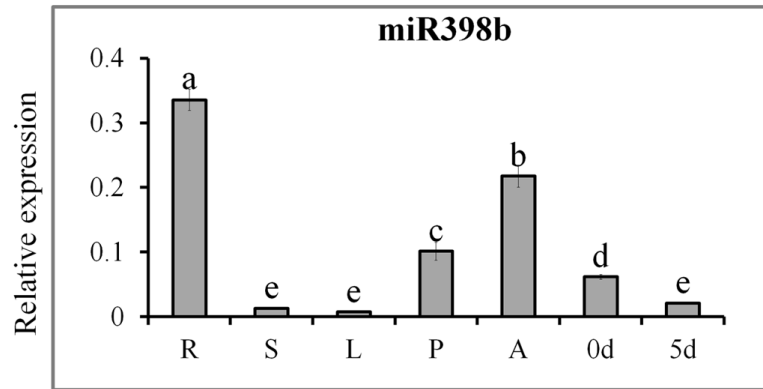
Zhang, D.D., Wang, J., Wang, D., Kong, Z.Q., Zhou, L., Zhang, G.Y., Gui, Y.J., Li, J.J., Huang, J.Q., Wang, B.L., Liu, C., Yin, C.M., Li, R.X., Li, T.G., Wang, J.L., Short, D.P.G., Klosterman, S.J., Bostock, R.M., Subbarao, K.V., Chen, J.Y. and Dai, X.F. (2019) Population genomics demystifies the defoliation phenotype in the plant pathogen *Verticillium dahliae* . *New Phytol* **222** , 1012-1029.

Zhang, H., Zhang, J., Yan, J., Gou, F., Mao, Y., Tang, G., Botella, J.R. and Zhu, J.K. (2017) Short tandem target mimic rice lines uncover functions of miRNAs in regulating important agronomic traits. *Proc Nat Acad Sci USA* **114** , 5277-5282.

Zhao, Y.L., Zhou, T.T. and Guo, H.S. (2016) Hyphopodium-specific VdNoxB/VdPls1-dependent ROS-Ca²⁺ signaling is required for plant infection by *Verticillium dahliae* . *PLoS pathog* **12** , e1005793.

Zhu, C., Ding, Y. and Liu, H. (2011) MiR398 and plant stress responses. *Physiol Plant* **143** , 1-9.

A



B

